

2014

Magnetic hardening of $Zr_2Co_{11}:(Ti, Si)$ nanomaterials

Wenyong Zhang

University of Nebraska-Lincoln, wenyong.zhang@unl.edu

Shah R. Valloppilly

University of Nebraska-Lincoln, svalloppilly2@unl.edu

Xingzhong Li

University of Nebraska-Lincoln, xli2@unl.edu

Yi Liu

University of Nebraska-Lincoln, yliu@unl.edu

Steven A. Michalski

University of Nebraska-Lincoln, smichalski2@unl.edu

See next page for additional authors

Follow this and additional works at: <http://digitalcommons.unl.edu/physicsellmyer>

 Part of the [Physics Commons](#)

Zhang, Wenyong; Valloppilly, Shah R.; Li, Xingzhong; Liu, Yi; Michalski, Steven A.; George, T A.; Skomski, Ralph A.; and Sellmyer, David J., "Magnetic hardening of $Zr_2Co_{11}:(Ti, Si)$ nanomaterials" (2014). *David Sellmyer Publications*. 278.
<http://digitalcommons.unl.edu/physicsellmyer/278>

This Article is brought to you for free and open access by the Research Papers in Physics and Astronomy at DigitalCommons@University of Nebraska - Lincoln. It has been accepted for inclusion in David Sellmyer Publications by an authorized administrator of DigitalCommons@University of Nebraska - Lincoln.

Authors

Wenyong Zhang, Shah R. Valloppilly, Xingzhong Li, Yi Liu, Steven A. Michalski, T A. George, Ralph A. Skomski, and David J. Sellmyer

Published in *Journal of Alloys and Compounds* 587 (2014), pp. 578–581;

doi: 10.1016/j.jallcom.2013.10.234

Copyright © 2013 Elsevier B.V. Used by permission.

Submitted October 9, 2013; revised October 29, 2013; accepted October 30, 2013; published online November 8, 2013.

Magnetic hardening of $Zr_2Co_{11}:(Ti, Si)$ nanomaterials

W. Y. Zhang,^{1,2} S. Valloppilly,² X. Z. Li,² Y. Liu,^{1,2} S. Michalski,^{1,2}

T. A. George,^{1,2} R. Skomski,^{1,2} and D.J. Sellmyer^{1,2}

1. Department of Physics and Astronomy, University of Nebraska, Lincoln, NE 68588, USA
2. Nebraska Center for Materials and Nanoscience, University of Nebraska, Lincoln, NE 68588, USA

Corresponding author – W. Y. Zhang, Nebraska Center for Materials and Nanoscience, University of Nebraska, 855 N. 16th Street, Lincoln, NE 68588, USA; 402-472-6818; email wenyong.zhang@unl.edu

Abstract

The role of Ti and Si additions in the magnetic hardening of rapidly quenched Zr_2Co_{11} -based nanomaterials has been investigated. Nanocrystalline $Zr_{17-x}Ti_xCo_{83}$ and $Zr_{18}Co_{82-y}Si_y$ are mainly composed of rhombohedral Zr_2Co_{11} and a small amount of orthorhombic Zr_2Co_{11} , hcp Co, and cubic Zr_6Co_{23} . Ti addition decreases the mean grain size of the magnetic phases, and thus increases coercivity and energy product from 1.6 kOe and 1.9 MGOe for $x = 0$ to 2.6 kOe and 3.9 MGOe for $x = 2$, respectively. Si addition enhances the anisotropy field of the hard phase which increases the coercivity but slightly decreases the magnetization. This work shows that Ti has a positive effect on energy product through refinement of structure.

Keywords: nanomaterial, nanostructure, magnetic hardening, magnetic property

1. Introduction

Zr_2Co_{11} is a good candidate for the development of rare-earth-free permanent magnets due to its relatively strong uniaxial anisotropy (11 Merg/cm³) and high Curie temperature (773 K).^[1,2] Rhombohedral Zr_2Co_{11} is a hard magnetic phase whose formation requires a high

cooling rate.^[3] However, the coercivity (< 3 kOe) of the pure Zr–Co alloys is too low to further increase energy product, and elemental addition is a feasible way to modify the structure and to improve the magnetic properties of Zr–Co alloys. It has been reported that the introduction of boron reduced the grain size of magnetic phases, increasing the coercivity of $Zr_{20}Co_{80}$ ribbons.^[4] Annealing leads to a further increase of the coercivity in $Zr_{18}Co_{80}B_2$, possibly due to the increase of the crystalline size of hard magnetic phase.^[5] The decrease of Zr concentration increased the content of the hard magnetic phase, refined the nanostructure, and thus enhanced the remanence, coercivity, and energy product of the Zr–Co alloys.^[3,6] In $Zr_{18-z}Si_zCo_{80}B_2$ ($z = 0 - 2$) ribbons, the substitution of Si for Zr increases the volume fraction of fcc Co, decreases the grain size of the magnetic phases, and results in an improvement of magnetic properties.^[7] Ti addition improves the magnetic properties of nanocrystalline Zr_2Co_{11} -based alloys because Ti suppresses the formation of Zr_2Co_{11} dendrites upon solidification.^[8] In Zr–Co–Si–B ribbons, Mo addition suppresses the formation of hcp Co and enhances the grain size of hard magnetic phase.^[1] The coercivity mechanism of Zr_2Co_{11} -based alloys may be of the domain-wall-pinning-type or reverse-domain nucleation type, depending on the preparation process.^[5,6] So far, the role of the Ti or Si addition in modifying structure and in magnetic hardening have remained unclear, including the site occupancies of Ti and Si. In order to clarify these issues, we have used melt spinning to fabricate nanocrystalline $Zr_{17-x}Ti_xCo_{83}$ and $Zr_{18}Co_{82-y}Si_y$, we show that Ti addition refines the grain size of Co and enhances the energy product. Si addition increases the anisotropy field of the hard phase, and thus coercivity.

2. Experimental methods

Ingots of $Zr_{17-x}Ti_xCo_{83}$ ($x = 0, 1, 2, 3, 4$) and $Zr_{18}Co_{82-y}Si_y$ ($y = 0, 1, 2, 4, 6$) were arc melted from high-purity elements in an argon atmosphere. The ribbons were made by ejecting molten alloys in a quartz tube onto the surface of a copper wheel with a speed of 40 m/s. The ribbons are about 2 mm wide and 50 μ m thick. The phase components were determined by a Rigaku D/Max-B X-ray diffraction (XRD) system with Cu Ka radiation. The Scherrer equation was used to estimate the mean grain size of magnetic phases, and nanostructure was imaged using a JEOL 2010 Transmission Electron Microscope (TEM). The hysteresis loops were measured by a Quantum Design Superconducting Quantum Interference Device magnetometer with fields up to 7 T. The thermomagnetic curves were measured by a Quantum Design Physical Property Measurement System at temperatures up to 1000 K, during the measurement, the applied field was parallel to the long direction of the ribbon.

3. Results and discussion

Figure 1 shows XRD patterns of $Zr_{17-x}Ti_xCo_{83}$ ($x = 0, 2, 4$) and $Zr_{18}Co_{82-y}Si_y$ ($y = 0, 3, 6$). $Zr_{17-x}Ti_xCo_{83}$ ($x \leq 2$) consists of rhombohedral Zr_2Co_{11} , orthorhombic Zr_2Co_{11} , and hcp Co. The values of lattice parameters a , c and cell volume of rhombohedral Zr_2Co_{11} for $x = 0$, determined from XRD pattern, are 4.688 Å, 25.088 Å, and 477.517 Å³, respectively, which are

in good agreement with the values reported in reference.^[9] The values of the lattice parameters a , c and cell volume of rhombohedral Zr_2Co_{11} for $x = 2$ are 4.672 Å', 24.387 Å', and 461.033 Å³, respectively. The cell volume decreases with increasing x , implying that the smaller Ti atoms occupy the sites of the larger Zr atoms. This is probably because the atomic radius (147 pm) of Ti is closer to that (160 pm) of Zr than that of Co (125 pm). The relative intensity of the diffraction peaks from orthorhombic Zr_2Co_{11} and hcp Co decreases with increasing x , indicating that Ti addition restrains the formation of orthorhombic Zr_2Co_{11} and hcp Co and favors the formation of rhombohedral Zr_2Co_{11} . The full width at half maximum of diffraction peaks of the magnetic phases increases with x , which means the mean grain size of the magnetic phases decreases. Further Ti addition ($x \geq 4$) leads to the formation of $(Zr,Ti)Co_{2.9}$ and increases the mean grain size of $Co(Ti)$. $Zr_{18}Co_{82-y}Si_y$ ($y \leq 3$) is comprised of rhombohedral Zr_2Co_{11} , orthorhombic Zr_2Co_{11} , cubic Zr_6Co_{23} , and hcp Co. The cell volume shrinks from 477.754 Å³ for $y = 0$ to 469.177 Å³ for $y = 3$, implying that Si enters Co site. This may be because the atomic radius (111 pm) of Si is closer to that (125 pm) of Co compared to Zr. The relative intensity of the diffraction peaks from Co decreases with increasing y , indicating that Si addition restrains the formation of Co and promotes the formation of the hard Zr_2Co_{11} phase. The content of hard phase increases with y . The mean grain size of magnetic phases remains approximately constant.

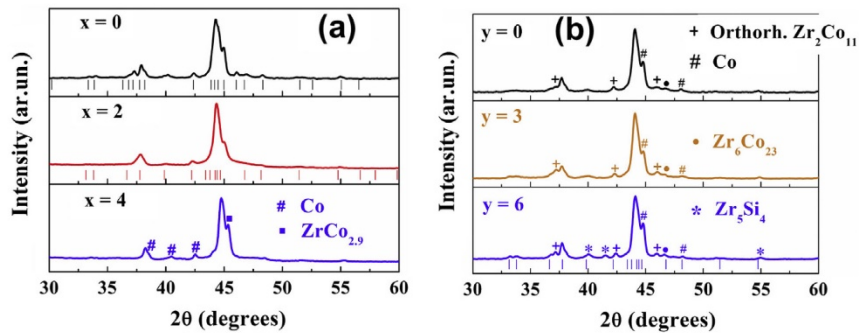


Figure 1. XRD patterns of $Zr_{17-x}Ti_xCo_{83}$ ($x = 0, 2, 4$) and $Zr_{18}Co_{82-y}Si_y$ ($y = 0, 3, 6$).

Figure 2 shows $M(T)$ curves of $Zr_{17-x}Ti_xCo_{83}$ ($x = 0, 2$) and $Zr_{18}Co_{82-y}Si_y$ ($y = 0, 2$). For $Zr_{17-x}Ti_xCo_{83}$ ($x = 0, 2$), three ferromagnetic-paramagnetic transitions were observed between 300 and 900 K. They correspond to rhombohedral Zr_2Co_{11} , orthorhombic Zr_2Co_{11} , and hcp Co, respectively. The Curie temperature of rhombohedral Zr_2Co_{11} is 755 K and is independent of x , suggesting that Ti occupies the Zr sites in rhombohedral Zr_2Co_{11} . For $Zr_{18}Co_{82-y}Si_y$ ($y = 0, 2$), the volume fraction of Zr_6Co_{23} was low so the magnetic signal was too weak to be detected. Only three phase transitions corresponding to rhombohedral Zr_2Co_{11} , orthorhombic Zr_2Co_{11} , and hcp Co appear in the $M(T)$ curves for the measured temperature range. The Curie temperature and magnetization of rhombohedral Zr_2Co_{11} decrease with y due to moment dilution and the weakening of the magnetic interaction. This implies that Si enters into the Co sites in rhombohedral Zr_2Co_{11} . The temperature-dependent drop in

magnetization with T for $y = 2$ is due to the ferro-paramagnetic transition of Co and orthorhombic Zr_2Co_{11} , which is significantly smaller than that for $y = 0$, indicating Si addition restrains the formation of Co and orthorhombic Zr_2Co_{11} and favors the formation of the hard phase. This agrees well with the XRD results.

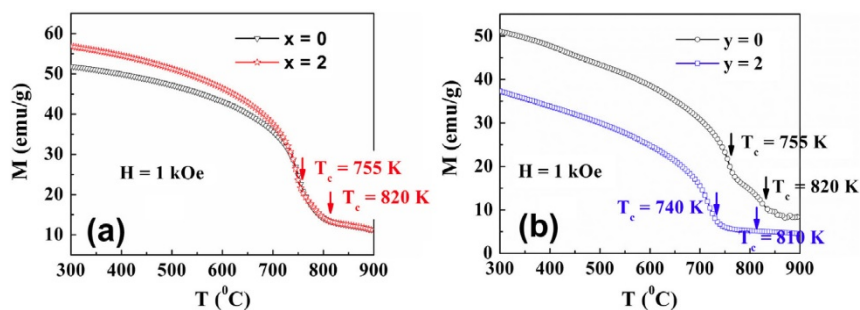


Figure 2. Thermomagnetic curves of $Zr_{17-x}Ti_xCo_{83}$ ($x = 0, 2$) and $Zr_{18}Co_{82-y}Si_y$ ($y = 0, 2$).

Figure 3 (a and b) shows hysteresis loops of $Zr_{17-x}Ti_xCo_{83}$ ($x = 0-4$) and $Zr_{18}Co_{82-y}Si_y$ ($y = 0-6$). Ti addition in limited amounts ($x \leq 2$) decreases the mean grain size of magnetic phases, which promotes more effective exchange coupling of the soft-magnetic phase. Therefore, the coercivity increases with x . The reason for the increase of the coercivity is that large and therefore poorly exchange-coupled soft regions switch easily. The remanence and squareness of the hysteresis loops are significantly enhanced (see fig. 3c). Therefore, the energy product increases from 1.9 MGOe for $x = 0$ to 3.9 MGOe for $x = 2$. The magnetocrystalline anisotropy constant K , and the saturation magnetization M_s of $Zr_{18}Co_{82-y}Si_y$ can be estimated using the law of the approach to saturation. The magnetocrystalline anisotropy field was calculated as $H_a = 2K/M_s$.^[10] The values of H_a for $y = 0, 4$, and 6 are 32.8, 39.5, and 45 kOe, respectively. Si addition increases the magnetocrystalline anisotropy field, leading to an enhancement of coercivity from 2.6 kOe for $y = 0$ to 4.1 kOe for $y = 4$ (see fig. 3d). Further Si addition ($y = 6$) results in the formation of nonmagnetic Zr_5Si_4 , which decreases the content of the hard phase and causes the coercivity to decrease. The magnetization decreases with y which leads to a decrease in the energy product. Based on the above results, it is expected that the combinatorial addition of Ti and Si will further improve magnetic properties.

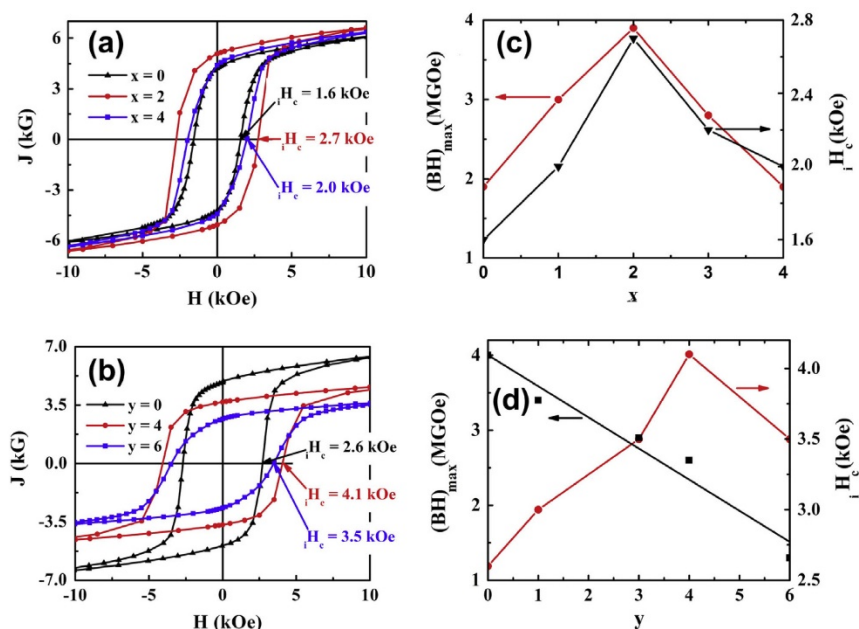


Figure 3. Hysteresis loops of (a) $Zr_{17-x}Ti_xCo_{83}$ ($x = 0-4$) and (b) $Zr_{18}Co_{82-y}Si_y$ ($y = 0-6$). The (c) and (d) are the deduced magnetic properties.

Figure 4 shows the TEM images of $Zr_{17-x}Ti_xCo_{83}$ ($x = 0, 2$), $Zr_{18}Co_{82-y}Si_y$ ($y = 0, 4$) and corresponding statistical distributions of the grain sizes for the magnetic phases. Compared to the $x = 0$ sample, the $x = 2$ sample has a more homogeneous and narrower grain-size distribution. The mean grain size of the magnetic phases decreases from 110 nm for $x = 0$ to 20 nm for $x = 2$. This indicates that Ti addition refines the nanostructure, in good agreement with the XRD results, and thus significantly improves the magnetic properties. The mean grain size for the $y = 4$ ribbon is almost the same as that for the $y = 0$ ribbon. But the $y = 4$ sample has narrower grain size distribution than the $y = 0$ sample, implying a more homogeneous nanostructure. This may be another reason leading to the enhancement of coercivity due to Si addition.

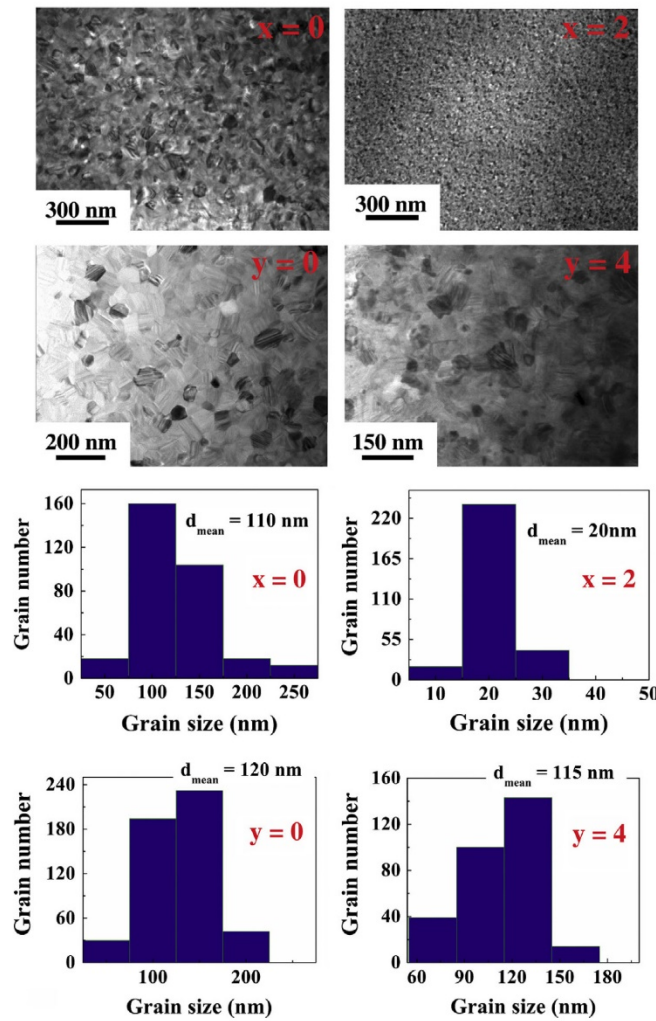


Figure 4. TEM images of $Zr_{17-x}Ti_xCo_{83}$ ($x = 0, 2$), $Zr_{18}Co_{82-y}Si_y$ ($y = 0, 4$) and corresponding statistical distribution of the grain size for $x = 0, x = 2, y = 0, y = 4$.

4. Conclusions

Ti and Si additions play a significant role in magnetic hardening in nanocrystalline Zr_2Co_{11} -based alloys. Ti addition shrinks the unit cell volume, but the Curie temperature of hard phase is unchanged, indicating Ti occupies Zr sites. Ti addition increases the volume fraction of the hard phase and decreases the mean grain size of the magnetic phases, thereby promoting effective exchange coupling to the soft phase and enhancing the remanence, coercivity, and energy product. Excessive Ti addition leads to the formation of $ZrCo_{2.9}$, which deteriorates the magnetic properties of $Zr_{17-x}Ti_xCo_{83}$. Si addition shrinks the unit cell volume and decreases the Curie temperature of the hard phase, implying that Si enters

into Co sites. Si addition restrains the formation of hcp Co and orthorhombic Zr_2Co_{11} , increases the volume fraction of hard phase, enhances the magnetocrystalline anisotropy field of hard phase, and thus leads to the significant increase of coercivity. Excessive Si addition yields nonmagnetic Zr_5Si_4 , which deteriorates the magnetic properties.

Acknowledgements – This work is supported by Department of Energy/BREM (DE-AC02-07CH11358, Subaward No. SC-10-343). It was carried out in part in the Central Facilities of the Nebraska Center for Materials and Nanoscience, which is supported by the Nebraska Research Initiative.

References

- [1] E. Burzo, R. Grössinger, P. Hundegger, H. R. Kirchmayr, R. Krewenka, R. Lemaire, *J. Appl. Phys.* 70 (1991) 6550.
- [2] W. Y. Zhang, S. Valloppilly, X. Z. Li, R. Skomski, J. E. Shield, D. J. Sellmyer, *IEEE Trans. Mag* 48 (2012) 3603.
- [3] W. Y. Zhang, X. Z. Li, S. Valloppilly, R. Skomski, J. E. Shield, D. J. Sellmyer, *J. Phys. D: Appl. Phys.* 46 (2013) 135004.
- [4] T. Saito, *Appl. Phys. Lett.* 82 (2003) 2305.
- [5] T. Saito, *IEEE Trans. Mag.* 40 (2004) 2919.
- [6] L. Y. Chen, H. W. Chang, C. H. Chiu, C. W. Chang, W. C. Chang, *J. Appl. Phys.* 97 (2005) 10F307.
- [7] H. W. Chang, C. F. Tsai, C. C. Hsieh, C. W. Shih, W. C. Chang, C. C. Shaw, *J. Magn. Magn. Mater.* 346 (2013) 74.
- [8] A. M. Gabay, N. N. Shchegoleva, V. S. Gaviko, G. V. Ivanova, *Phys. Met. Metall.* 95 (2003) 16.
- [9] G. V. Ivanova, N. N. Shchegoleva, A. M. Gabay, *J. Alloys Comp.* 432 (2007) 135.
- [10] D. J. Sellmyer, Y. F. Xu, M. L. Yan, Y. C. Sui, J. Zhou, R. Skomski, *J. Magn. Magn. Mater.* 303 (2006) 302.